

# Supplemental Data

Pei *et al.*,

Paracellular epithelial transport maximizes energy efficiency in the kidney

---

Supplemental figures, Fig. S1-S17

Supplemental tables, Table S1-S3

Supplemental References

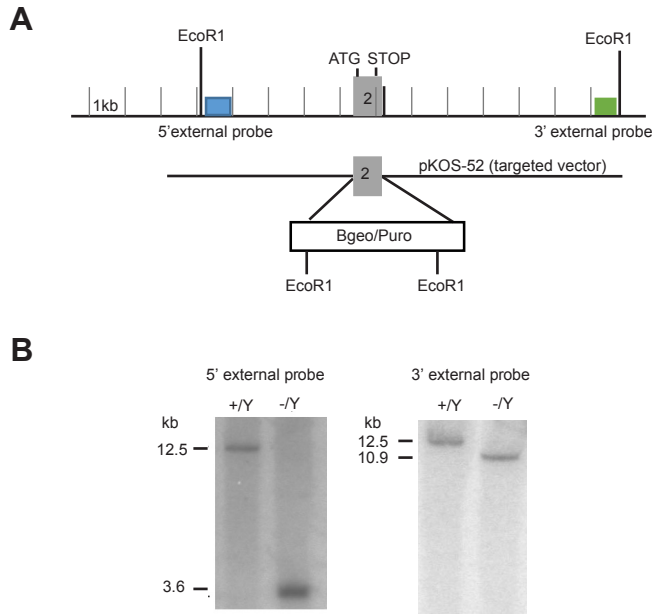


**Figure S1.** Generation of claudin-2 knockout mice. **A.** Diagram of targeting strategy. The grey bar indicates the single coding exon of the mouse claudin-2 gene. The targeting vector contains a  $\beta$ Geo/Puro cassette designed to replace all of the coding region and part of the 3'-UTR. The 5' external probe is indicated by the green bar and the 3' external probe by the blue bar. From mmrc.mouse biology.org (Lexicon Genetics MEM726N1). **B.** Southern blot of EcoR1-digested genomic DNA from wild-type (+/Y) and hemizygous (-/Y) mice indicates correct targeting. Blotting using the 5' external probe indicated in A. should yield a 12.5 kb or a 3.6 kb band from the wild-type and targeted allele, respectively. Blotting with the 3' external probe should yield a 12.5 kb or a 10.9 kb band from the wild-type and targeted allele, respectively.

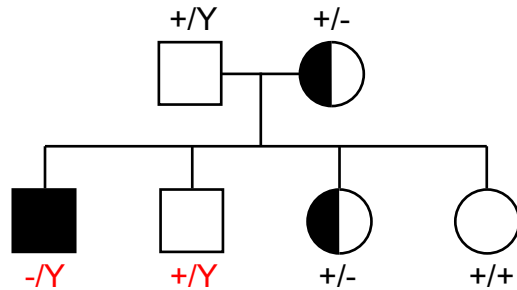
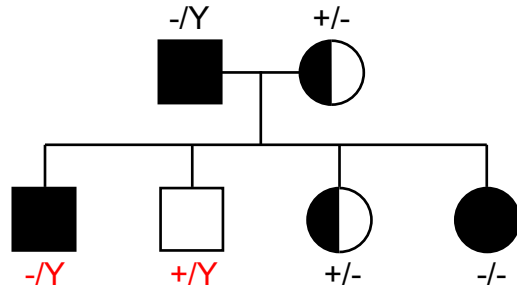


**Figure S2.** Two breeding strategies used to generate the matched WT  $[+/Y]$  and KO  $[-/Y]$  littermates (red labels) used for the experiments described. Genotypes refer to alleles at the claudin-2 locus on the X chromosome. Fully shaded symbols are mice that are claudin-2 null, partially shaded symbols represent heterozygotes.

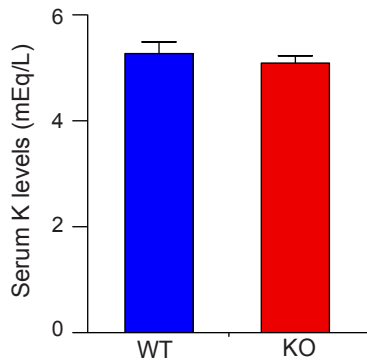


**Figure S3.** Serum potassium (K) concentration in claudin-2 WT and KO mice, in mEq/L (n = 6 mice per group,  $p = \text{NS}$ ).

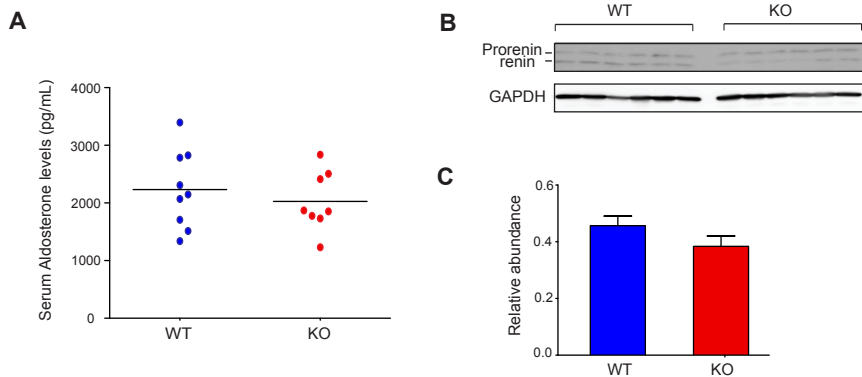


**Figure S4.** Renin and aldosterone levels in claudin-2 WT and KO mice. **A.** Serum aldosterone levels ( $p = \text{NS}$ ). **B.** Upper panel: Western blot of the whole kidney lysates probed with a renin antibody, showing distinct bands for prorenin and renin. Lower panel: Immunoblot for GAPDH as a loading control. **C.** Quantitation of the blots depicted in B. Relative protein abundance (renin + prorenin)/GAPDH is presented as mean  $\pm$  S.E.M. ( $p = 0.04$ ).

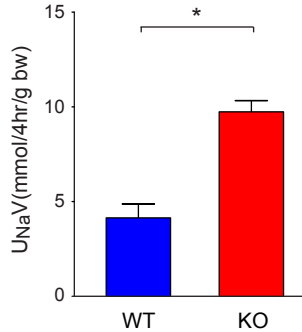


**Figure S5.** Hypertonic saline challenge test. Mice were given 40 mL/kg bw of 2% (wt/vol) NaCl i.p. and urine collected over the subsequent 4 h. Urine Na excretion (U<sub>Na</sub>V) was greater in KO mice than WT. \* $p < 0.01$  (n = 5 WT and 4 KO).

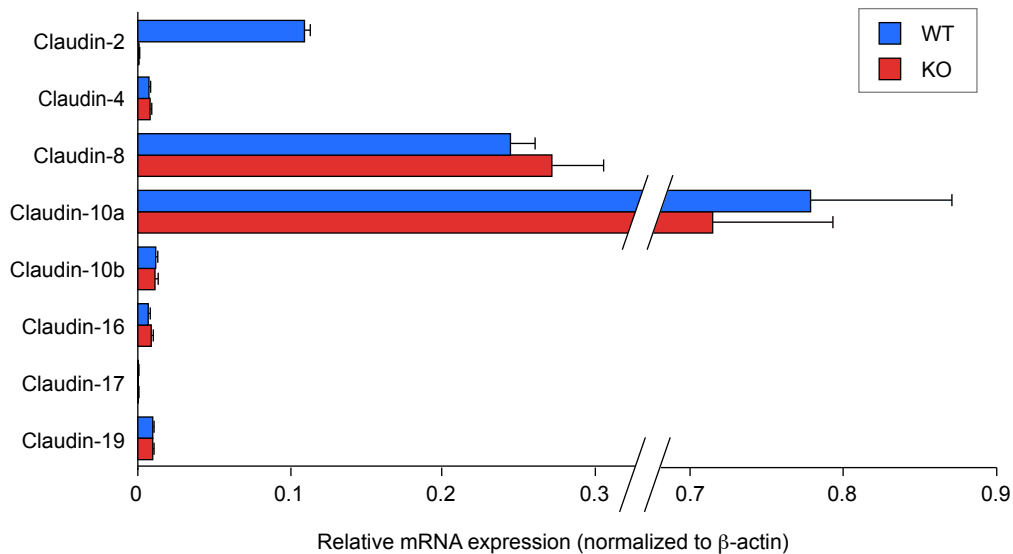


**Figure S6.** Claudin mRNA expression in claudin-2 WT and KO mouse kidneys, quantitated by real-time RT-PCR and normalized to the level of  $\beta$ -actin by the  $\Delta$ Ct method (n = 6 per group).

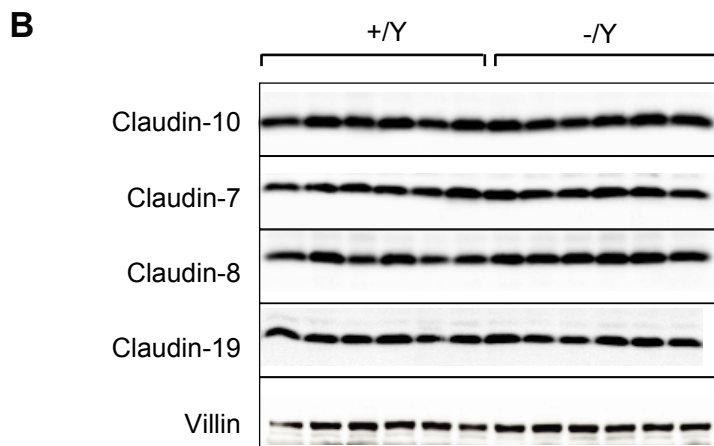
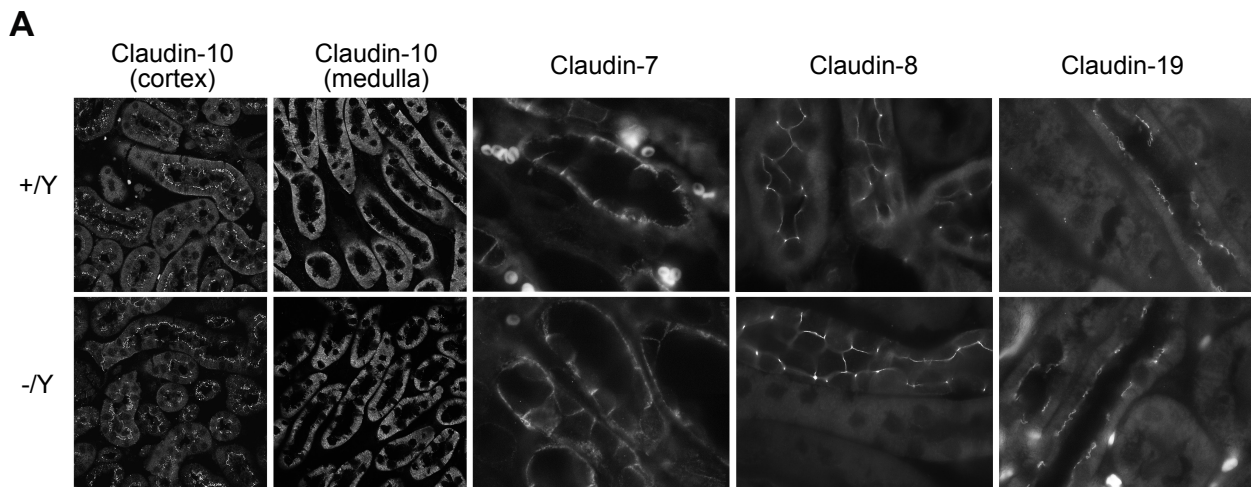


**Figure S7.** Protein expression and localization of claudin isoforms in the *Cldn2* [+ $\gamma$ ] and *Cldn2* [- $\gamma$ ] mice. **A.** Immunolocalization of claudin isoforms. Mouse kidney frozen sections were stained with claudin-10, claudin-7, claudin-8, and claudin-19 antibodies. **B.** Western blot of whole kidney lysates probed with mouse anti-claudin-10, claudin-7, claudin-8, claudin-19 antibodies showing bands at the expected sizes. The lower panel shows an immunoblot for villin as a loading control.

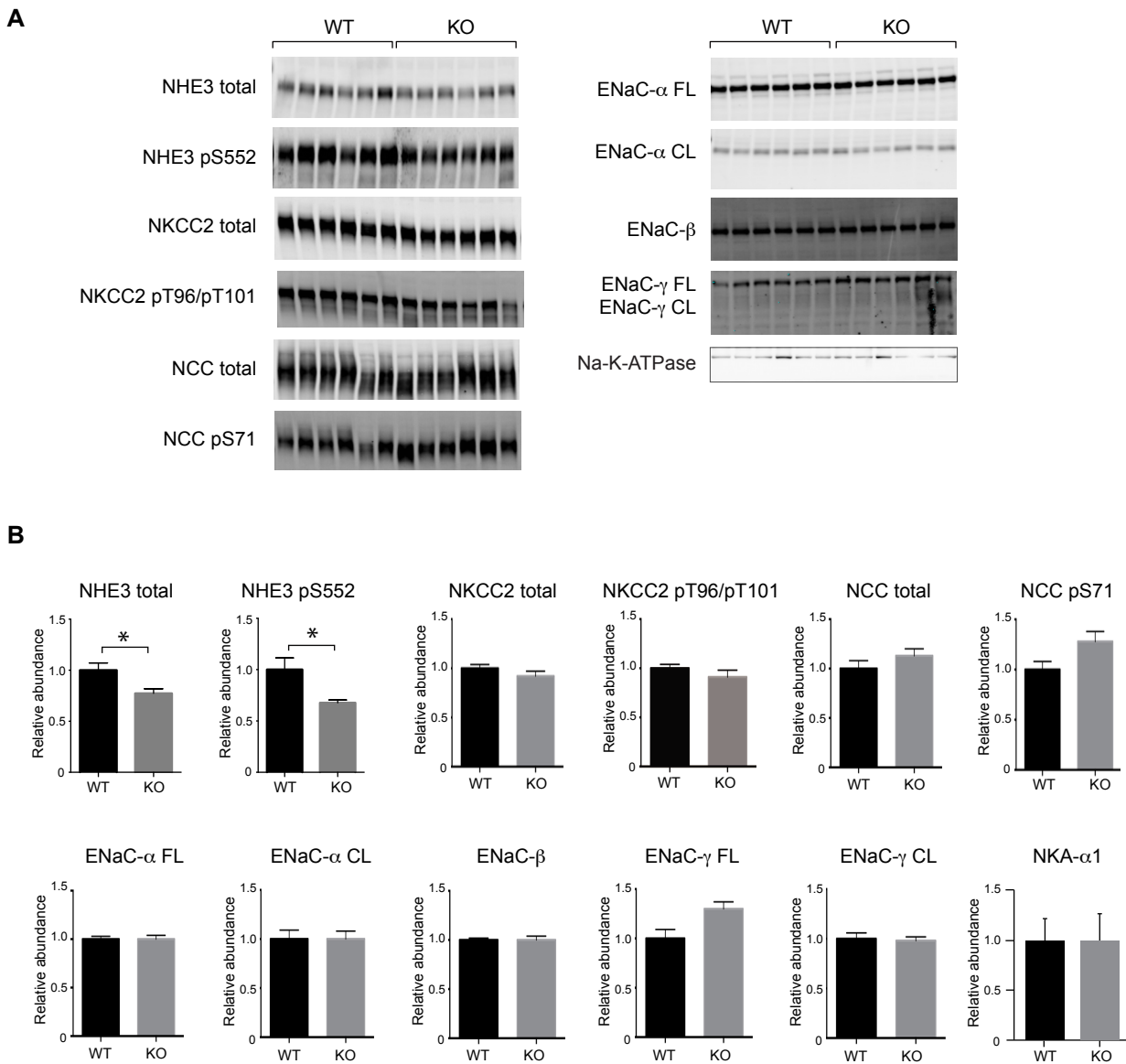


**Figure S8.** Expression of renal transcellular Na transport proteins. **A.** Immunoblots of whole kidney lysates with antibodies to total or phosphorylated Na-H exchanger (NHE3), thiazide-sensitive electro-neutral NaCl cotransporter (NCC), apical Na-K-2Cl cotransporter (NKCC2) and the 3 subunits of the epithelial Na channel (ENaC- $\alpha$ , - $\beta$  and - $\gamma$ ), and Na-K-ATPase  $\alpha$ 1 subunit (NKA- $\alpha$ 1). FL, full-length; CL, cleaved. **B.** Results of quantitation of the immunoblot band densities as a measure of protein abundance which are displayed as individual records with mean  $\pm$  SEM. \* $p < 0.05$ .

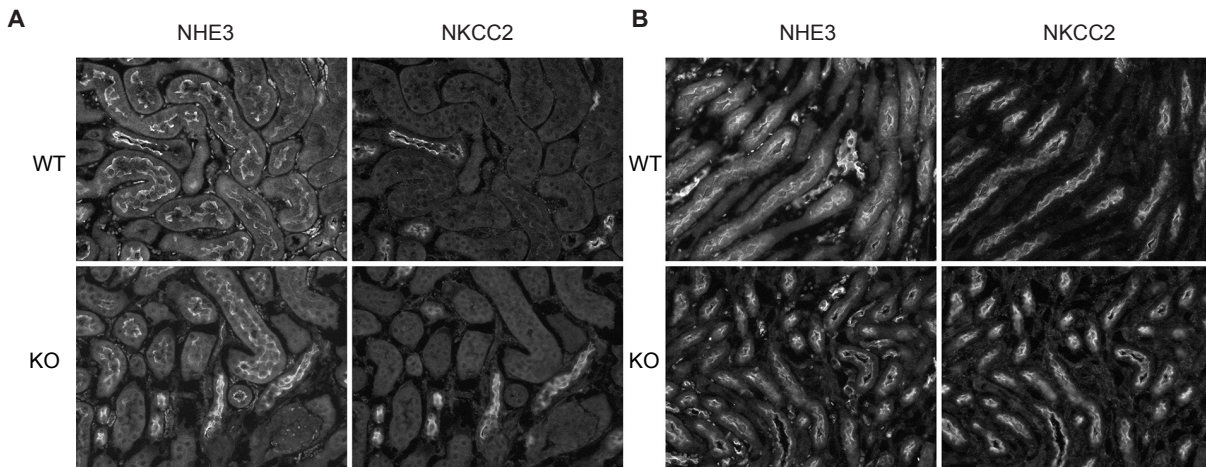


**Figure S9.** Immunofluorescence staining of Na/H exchanger-3 (NHE3) antigen in the renal cortex and medulla. Claudin-2 WT and KO kidneys were perfusion-fixed and cryosections stained for NHE3 or NKCC2. Representative pictures of cortex (**A**) and medulla (**B**) showed similar NHE3 expression between WT and KO, both in tubules that do not express NKCC2 (PT S1 and S2 in cortex, S3 and thin descending limbs in medulla), and in tubules that coexpress NKCC2 (cortical and medullary TALH). Images are representative of findings from 3 mice per group.

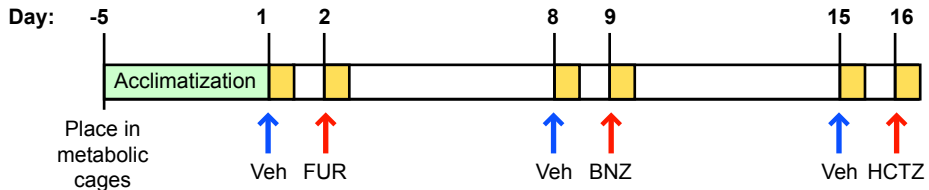


**Figure S10.** Timeline of the diuretic challenge experiment. Yellow boxes denote 4 hr urine collection. Blue arrows indicate i.p. injection of the appropriate vehicle (Veh), either saline or methanol. Red arrows indicate i.p. injection of diuretic: FUR, furosemide; BNZ, benamil; HCTZ, hydrochlorothiazide.

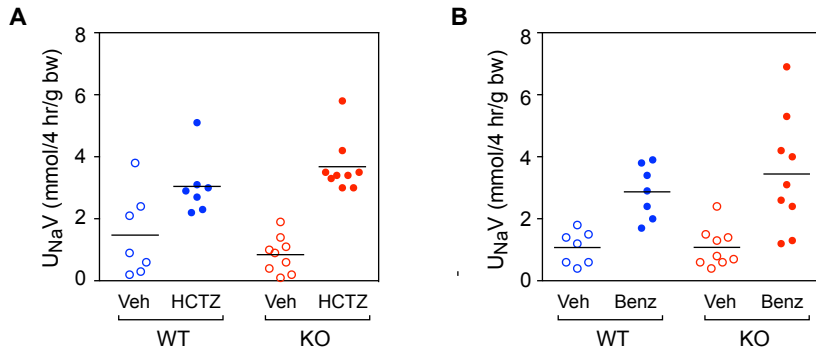


**Figure S11.** Absence of compensatory increase in the activity of NCC and ENaC in claudin-2 KO mice, as determined by diuretic challenge. NCC and ENaC activity in WT and KO mice were assessed by measuring the natriuretic response over 4 hr after a single i.p. bolus of hydrochlorothiazide (HCTZ, an NCC blocker, 25 mg/kg) or benzamil (Benz, an ENaC blocker, 1.4 mg/kg), or matching vehicle (Veh) ( $n = 8$  per group). Circles represent individual measurements and horizontal lines indicate the group means.

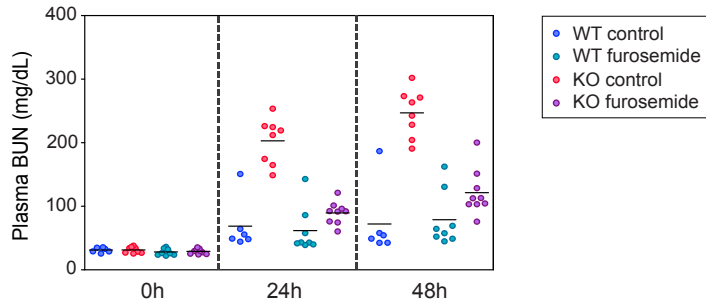


**Figure S12.** Effect of claudin-2 KO on susceptibility to acute renal ischemia. BUN levels measured at 0, 24, and 48 hours following bilateral renal IRI in claudin-2 KO and wildtype littermates with/without furosemide pre-treatment. Individual-level data shown here in dot plots are from the experiment summarized in Fig. 5A of the main text.

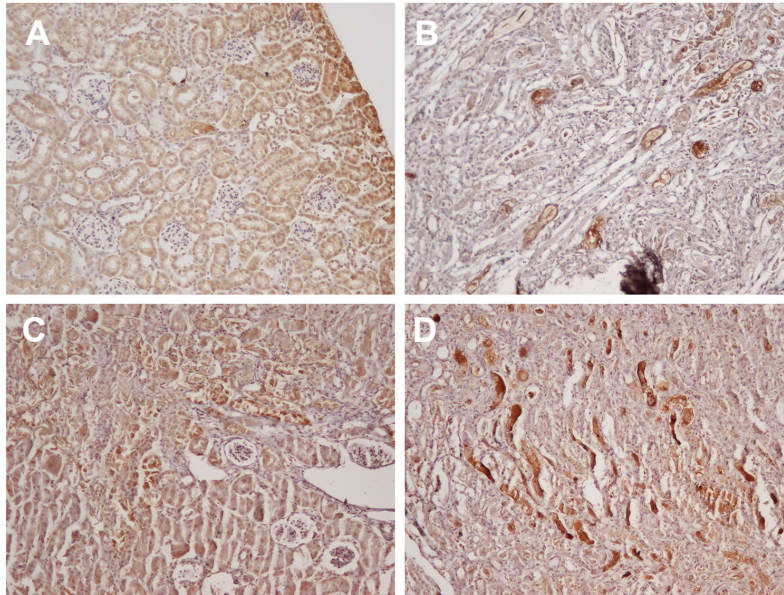


**Figure S13.** Confirmation of kidney injury by KIM-1 protein staining. Representative images are shown of rabbit anti-KIM-1 antibody immunohistochemistry staining of the kidney cortex (A, C) and outer medulla (B, D) from WT (A, B) and KO (C, D) mice 48 hr following IRI.

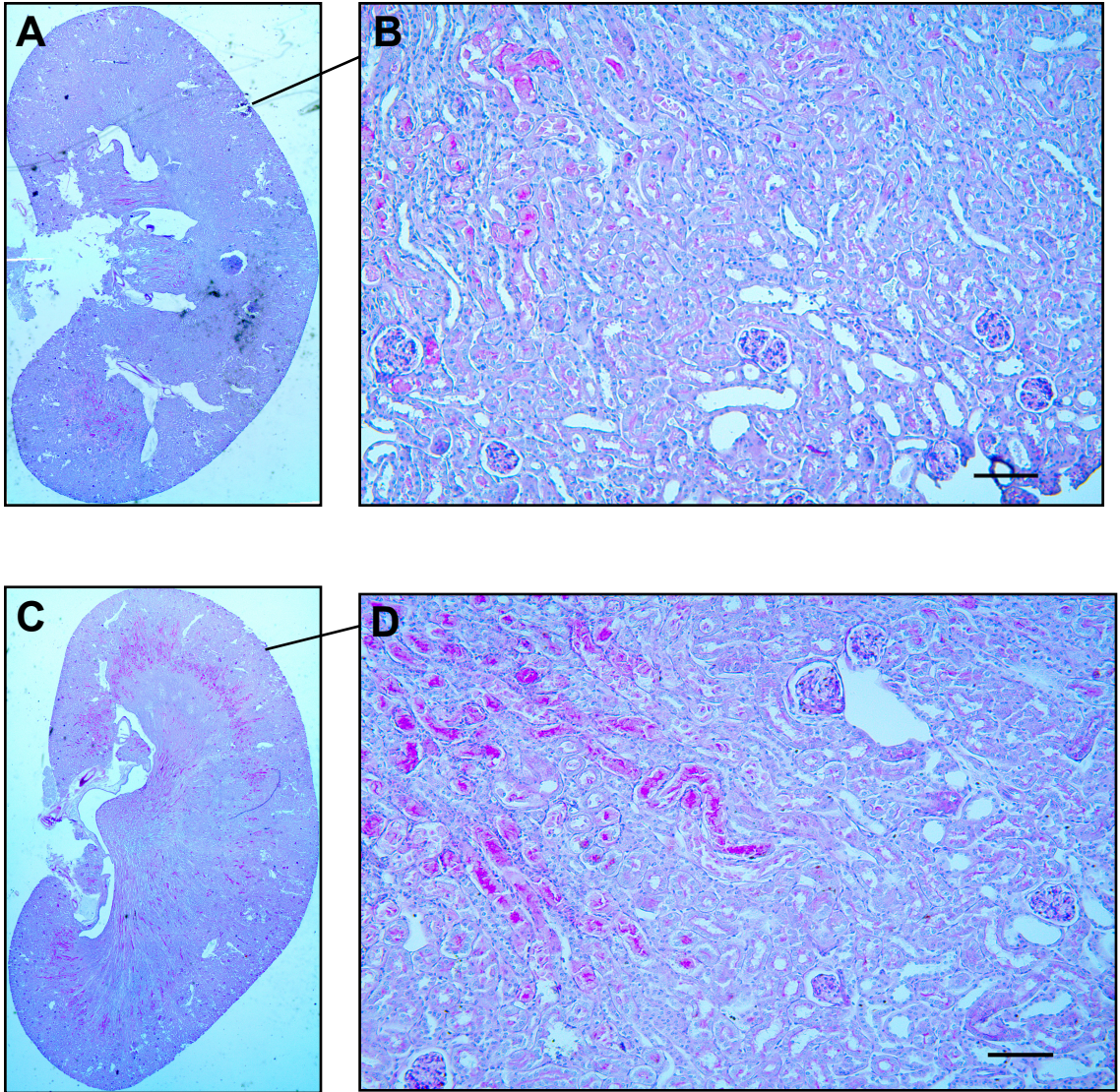


**Figure S14.** Histological analysis of acute kidney injury in mice pretreated with furosemide. Representative images are shown of periodic acid-Schiff (PAS)-stained WT (**A, B**) and KO (**C, D**) kidneys 48 hrs following IRI. **A, C** are low power overviews of the whole kidney section. **B, D** are higher power views showing the cortex and outer medulla (100  $\mu\text{m}$  scale bar). Please see Fig. 6 in the main text for quantitative scoring of the degree of injury.

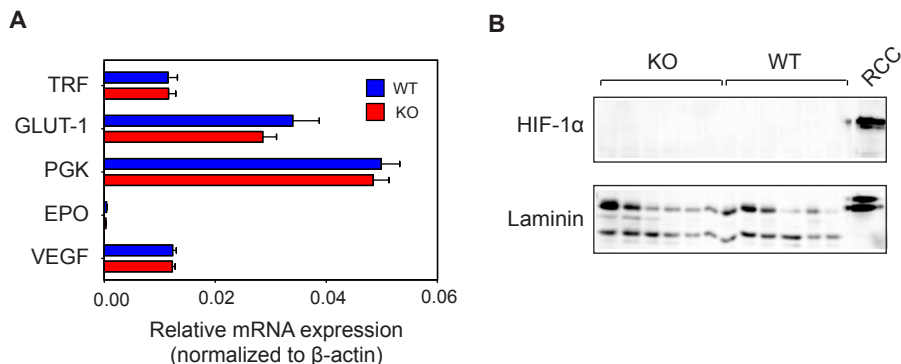


**Figure S15.** Absence of HIF-1 $\alpha$  activation in claudin-2 KO kidney. **A.** Quantification of whole kidney mRNA levels of HIF-1 $\alpha$  target genes in claudin-2 WT and KO mice, normalized to  $\beta$ -actin expression. TRF, transferrin; GLUT-1, glucose transporter 1; PGK, phosphoglycerate kinase; EPO, erythropoietin; VEGF, vascular endothelial growth factor. The fold change is presented as mean  $\pm$  S.E.M. **B.** Western blots of nuclear fractions of kidney tissue from WT and KO mice. Upper panel is probed with rabbit anti-HIF-1 $\alpha$  antibody. The last lane contains human renal cell carcinoma lysate (RCC) as a HIF-1 $\alpha$  expression positive control. There is absence of HIF-1 $\alpha$  in both WT and KO kidney at baseline. Lower panel shows the same blot stripped and reprobbed with rabbit anti-laminin as a marker for nuclear proteins.

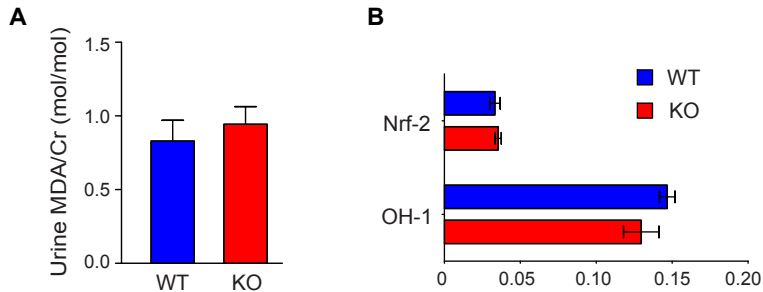


**Figure S16.** Absence of increased oxidative stress in claudin-2 KO kidneys compared to WT kidneys at baseline. **A.** Urinary malondialdehyde (MDA) excretion was expressed as the ratio of urinary MDA concentration to creatinine concentration (mean  $\pm$  S.E.M.). **B.** mRNA expression of oxidative stress response genes. Quantification of whole kidney mRNA levels of OH-1 and Nrf2 gene relative to  $\beta$ -actin. OH-1, heme oxygenase 1; Nrf2, nuclear factor, erythroid-derived 2. The fold change is presented as mean  $\pm$  S.E.M.

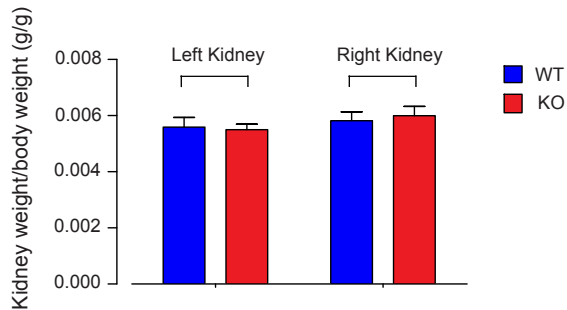


**Figure S17.** Kidney weight of claudin-2 WT and KO mice. Kidney weight is represented as the ratio between left or right kidney weight and body weight.

**Table S1.** Oligonucleotide primers that were used for genomic DNA or quantitative RT-PCR

$\beta$ -Actin Forward	5'-CTA AGG CCA ACC GTG AAA AG-3'
$\beta$ -Actin Reverse	5'-ACC AGA GGC ATA CAG GGACA-3'
Claudin 2 Forward	5'-TGGCGTCCAACCTGGTGGGCT-3'
Claudin 2 Reverse	5'-ACCGCCGTCACAATGCTGGC-3'
Claudin 4 Forward	5'-TGGGGACAGGCAAACCCGGA-3'
Claudin 4 Reverse	5'-CTTGCCGGCCGTAAGGAGCC-3'
Claudin 8 Forward	5'-TCCCTGTCAGCTGGGTTGCCA-3'
Claudin 8 Reverse	5'-GCTCGCGCTTTAGGGCCACA-3'
Claudin 10b Forward	5'-GAT CTG CGT TAC CGA TTC CA-3'
Claudin 10b Reverse	5'-GCA GCG ATC ATT AGT CCT CTA C-3'
Claudin 16 Forward	5'-GCA AGA GGG ATG TGA GGA AA-3'
Claudin 16 Reverse	5'-CTA TGG GCC TCT GTT GCT ATT-3'
Claudin 17 Forward	5'-GAC TCC TAC ACA TTC TGC ATCT-3'
Claudin 17 Reverse	5'-CCA GCG ATC TGT AAG GGA TAAA-3'
Claudin 19 Forward	5'-GAA GGA AGA GTG TGG GAG AAAC-3'
Claudin 19 Reverse	5'-GAG CCT TCA GCC TTG AGA TTAG-3'
KIM-1 Forward	5'-CAG GAA GAC CCACGACTA TTTC-3'
KIM-1 Reverse	5'-GTG TGT AGA TGT TGG AGG AGTG-3'
Cyclophilin B Forward	5'-CGA GTC GTC TTT GGA CTC TTT-3'
Cyclophilin B Reverse	5'-GCC AAA TCC TTT CTC TCC TGT A-3'
OH-1 Forward	5'-CTC CCT GTG TTT CCT TTC TCT C-3'
OH-1 Reverse	5'-GCT GCT GGT TTC AAA GTT CAG-3'
Nrf2 Forward	5'-CTC CGT GGA GTC TTC CAT TTA C-3'
Nrf2 Reverse	5'-GCA CTA TCT AGC TCC TCC ATT TC-3'
VEGF-A Forward	5'-CCA CGT CAG AGA GCA ACA TCA-3'
VEGF-A Reverse	5'-TCA TTC TCT CTA TGT GCT GGC TTT-3'
GLUT-1 Forward	5'-ATG GAT CCC AGC AGC AAG-3'
GLUT-1 Reverse	5'-CCA GTG TTA TAG CCG AAC TGC-3'
PGK Forward	5'-GGA AGC GGG TCG TGA TGA-3'
PGK Reverse	5'-GCC TTG ATC CTT TGG TTG TTT G-3'
TRF Forward	5'-TGG AGA CAG ATG CTC CCT CC-3'
TRF Reverse	5'-TTT GTG CTC TGT GTA TGT GGT AAG G-3'
EPO Forward	5'-CAT CTG CGA CAG TCG AGT TCT G-3'
EPO Reverse	5'-CAC AAC CCA TCG TGA CAT TTT C-3'
Claudin 2 genotype WT Forward	5'-CAGGCTCCGAAGATACTTC-3'
Claudin 2 genotype WT Reverse	5'-GTAGAAGTCCCGAAGGATG-3'
Claudin 2 genotype KO Reverse	5'-CCCTAGGAATGCTCGTCAAGA-3'

**Table S2.** Primary antibodies used for immunoblotting and immunofluorescence

Antibody Target	Apparent Mobility (kDa)	Protein ( $\mu\text{g}/\text{lane}$ )*	Primary antibody supplier (cat. no.)	Primary antibody host	Primary antibody dilution	Incubation time	Refs.
Claudin-2	23	10	ThermoFisher Scientific (#32-5600)	Mouse	1:2000	O/N	
Claudin-7	23	15	ThermoFisher Scientific (#34-9100)	Rb	1:1000	O/N	
Claudin-8	23	15	ThermoFisher Scientific (#40-2600)	Rb	1:500	O/N	
Claudin-10	21	15	ThermoFisher Scientific (#38-8400)	Rb	1:250	O/N	
Claudin19	23	15	Alan Yu (Univ. of Kansas)	Rb	1:1000	O/N	[1]
ENaC- $\alpha$	90 (full length), 25 (cleaved)	40, 20	Johannes Loffing (Univ. of Zurich)	Rb	1:5000	O/N	[2]
ENaC- $\beta$	100	30, 10	Johannes Loffing (Univ. of Zurich)	Rb	1:15000	O/N	[2]
ENaC- $\gamma$	80-60	40, 20	Lawrence Palmer (Cornell University)	Rb	1:5000	O/N	[3]
NCC	150	40, 20	Alicia McDonough (USC Keck)	Rb	1:5000	O/N	[4]
NCC pS71	150	40, 20	Johannes Loffing (Univ. of Zurich)	Rb	1:5000	2 hrs	[5]
NHE3	83	40, 20	Millipore	Rb	1:1000	O/N	
NHE3 pS552	85	40,20	Santa Cruz	Mu	1:1000	2 hrs	
NKCC	150	20, 10	Christopher Lytle "T4" (Univ. of California at Riverside)	Mu	1:6000	O/N	[6]
NKCC2pT96/pT101	150	20, 10	Biff Forbush "R5" (Yale University)	Rb	1:2000	2 hrs	[7]
Renin	37	30	AnaSpec (#54373)	Rb	1:1000	O/N	
HIF-1 $\alpha$	150	30	Novus (#NB100-449)	Rb	1:1000	O/N	
Lamin A/C	70-28	30	Cell Signaling (#2032)	Rb	1:1000	O/N	
Na <sup>+</sup> /K <sup>+</sup> -ATPase $\alpha$ subunit	100	6	Santa Cruz (#48345)	Mu	1:1000	O/N	
$\beta$ -actin	42	15	Sigma-Aldrich (#A2066)	Rb	1:4000	O/N	
Villin	90	15	Santa Cruz (#28283)	Rb	1:500	O/N	

\*Where two amounts are shown, this indicates that protein was loaded at two dilutions, differing by 2-fold, in different lanes to check for linearity.

ENaC, epithelial Na channel; NCC, thiazide-sensitive electroneutral NaCl cotransporter; NKCC, Na-K-2Cl cotransporter; pS/Tn, phosphorylated serine or threonine at position *n*; O/N, overnight.

**Table S3.** Primary antibodies used for immunofluorescence and immunohistochemistry

<b>Antibody Target</b>	<b>Primary antibody supplier (cat. no.)</b>	<b>Primary antibody host</b>	<b>Primary antibody dilution</b>	<b>Incubation time</b>
Claudin-2	ThermoFisher Scientific (#32-5600)	Mouse	1:500	O/N
Claudin-7	ThermoFisher Scientific (#34-9100)	Rb	1:500	O/N
Claudin-8	ThermoFisher Scientific (#40-2600)	Rb	1:200	O/N
Claudin-10	ThermoFisher Scientific (#38-8400)	Rb	1:100	O/N
Claudin-19	Alan Yu (Univ. of Kansas)	Rb	1:1000	O/N
NHE-3	Alicia McDonough (USC Keck)	Rb	1:1000	O/N
Kim-1	Novus (#NBP1-76701)	Rb	1:500	O/N
ZO-1	ThermoFisher Scientific, anti-ZO-1 Alexa Fluor® 594 conjugate (# 339194)	Mouse	1:1000	O/N

## Supplemental References

1. Angelow, S., et al., *Renal localization and function of the tight junction protein, claudin-19*. Am J Physiol Renal Physiol, 2007. **293**(1): p. F166-77.
2. Duc, C., et al., *Cell-specific expression of epithelial sodium channel alpha, beta, and gamma subunits in aldosterone-responsive epithelia from the rat: localization by in situ hybridization and immunocytochemistry*. The Journal of cell biology, 1994. **127**(6 Pt 2): p. 1907-21.
3. Ergonul, Z., G. Frindt, and L.G. Palmer, *Regulation of maturation and processing of ENaC subunits in the rat kidney*. American journal of physiology. Renal physiology, 2006. **291**(3): p. F683-93.
4. Nguyen, M.T., et al., *Differential regulation of Na<sup>+</sup> transporters along nephron during ANG II-dependent hypertension: distal stimulation counteracted by proximal inhibition*. American journal of physiology. Renal physiology, 2013. **305**(4): p. F510-9.
5. Picard, N., et al., *Protein phosphatase 1 inhibitor-1 deficiency reduces phosphorylation of renal NaCl cotransporter and causes arterial hypotension*. Journal of the American Society of Nephrology : JASN, 2014. **25**(3): p. 511-22.
6. Lytle, C., et al., *Distribution and diversity of Na-K-Cl cotransport proteins: a study with monoclonal antibodies*. The American journal of physiology, 1995. **269**(6 Pt 1): p. C1496-505.
7. Flemmer, A.W., et al., *Activation of the Na-K-Cl cotransporter NKCC1 detected with a phospho-specific antibody*. The Journal of biological chemistry, 2002. **277**(40): p. 37551-8.